Utilising SMC in Single Phase Permanent Magnet Linear Motors for Compressor Applications

Z.S. Al-Otaibi, A.G. Jack

Merz court, Newcstle university,Newcastle upon Tyne, NE1 7RU
zalotaibi@yahoo.com, alan.jack@ncl.ac.uk

Keywords: linear motors, single phase, SMC, flexure springs, resonance.

Abstract

This paper aims to present the design and the construction of a new geometry using an SMC core in a single phase permanent magnet linear motor with a flux concentrating buried magnet arrangement. It also presents running test results from the prototype.

1 Introduction

The increasing attention being attracted to all matters concerning energy and the environment are creating strong drivers for improved energy efficiency. Cooling systems are large users of electrical energy. Linear oscillating permanent magnet drives for the piston compressors used in domestic refrigerators look promising compared to the current crank mechanism as they eliminate the two bearings used in the crank, have the possibility to remove bearings for the motor and employ much higher efficiency permanent magnet technology without the need for complex electronics. In these systems springs are used to make them resonant at the supply frequency. The net result is a system which will self-start and can be driven using only voltage magnitude control techniques (for instance using just triacs). This style of machine is hardly new with what might be the first reference as early as 1908 [1]. In recent years however they have attracted renewed interest [2-6] and commercialisation [3]. In these machines the stator core carries oscillating fields and hence needs to be subdivided to avoid very high eddy current loss. Using laminations to achieve this subdivision requires that the laminations lie in a radial/axial plane which causes severe difficulties in construction due to the "wedge shape" into which the laminations fit. This seems to form an ideal application for cores constructed from compacted insulated iron powder or soft magnetic composite (SMC) as it has become known. SMC has isotropic magnetic properties and this not only easily accommodates the basic field directions required but also allows a large number of alternate designs to be considered [5, 6].

2 Design

The geometry of the motor considered here employs a single phase winding in the form of a simple hoop coil. The stator is formed from two hollow rings pressed from SMC. The rotor uses a flux concentrating buried magnet arrangement using two magnets which are simple rings magnetised in the axial direction. This geometry has been chosen for the strength of the mover, its ease of production and the low magnet cost [6]. Early and final designs of the geometry are shown in Fig. 1 which shows a solution from the axi-symmetric finite element model which has been used to analyse the machine.

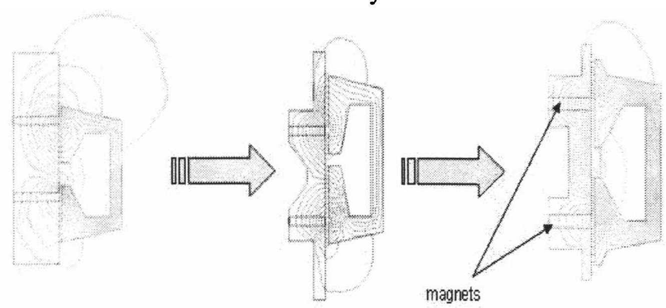

Figure 1: Stages of the geometry

The system should be resonant at supply frequency; clearly this means that the heavier the mover the more spring stiffness is necessary. A simple system employs helical springs supported by linear bearings. This might be compared with a flexure spring system which is used here which integrates the springs and bearings in one part [7]. The required stiffness, the relatively large movement and adequate fatigue life are difficult to achieve. One of the outcomes of this prototype is the testing of the spring system. The solution chosen is for 7 springs per side of each motor. One of the springs is shown in Fig. 2. The stress relieving holes and the slightly off–helical slot that have been derived to reduce stress concentrations and hence improve fatigue life may be noted from this figure.

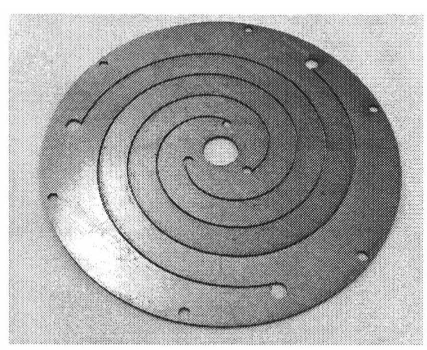

Figure 2: Single flexure spring

3 Motor Construction

The test system is two machines mechanically connected in a back to back arrangement (one generator, one motor). To build the two machines, four stator cups and eight mover sections have been machined from standard green blanks of Somaloy® 700 +0.4% Kenolube SMC compacted at 800 MPa [8]. All parts were then heat treated. The blanks were used here because they are preferred for prototyping as dies are expensive. Machining in the green state (i.e. after compaction but before heat treatment) and subsequently heat treating has been found to minimise the damage to the properties of the compact caused by machining.

Nonmagnetic steel has been used to construct the shaft. The shaft is hollow shaft to reduce the weight of the mover as much as possible.

The bobbin style coil is simple to machine wind using an s shaped former to create parallel/tapered cross section (see Fig. 1). The coils were constructed to both ends of the wire at the middle of the OD to be taken out from a small slot in the contact surface between the two cups.

Position and force need to be measured and the sensors weight and size are very important issues in their choice. Therefore, tension/compression load cell and Linear Variable Differential Transformer (LVDT) with a total weight of less than 50g both have been chosen to be used in the test rig.

Four rings of NdFeB with grade of 38H magnetised axially and Zinc primer plated have been used for the magnets in the machines.

The two SMC stator halves (one with the coil in place), the four SMC mover sections and the two "washer" shaped magnets are shown together with the force sensor in Fig. 3.

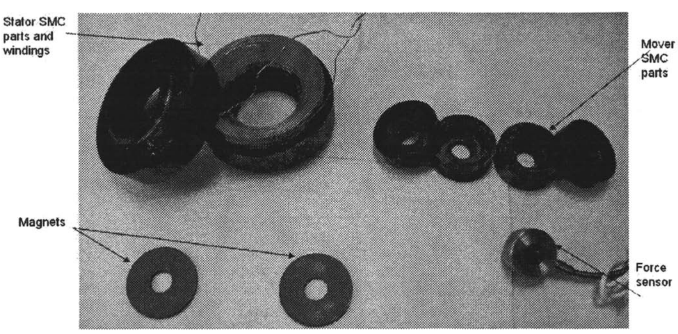

Figure 3: motor components, with case and force sensor

An outer case also was constructed to hold the stator halves and anchor the flexure springs. Fig. 4 shows the case, spring stacks, and the shaft with its sleeves.

Fig. 5 shows the most difficult step of the assembling process which is accommodating the mover into the case whilst maintaining the air gap between the magnets and the stator.

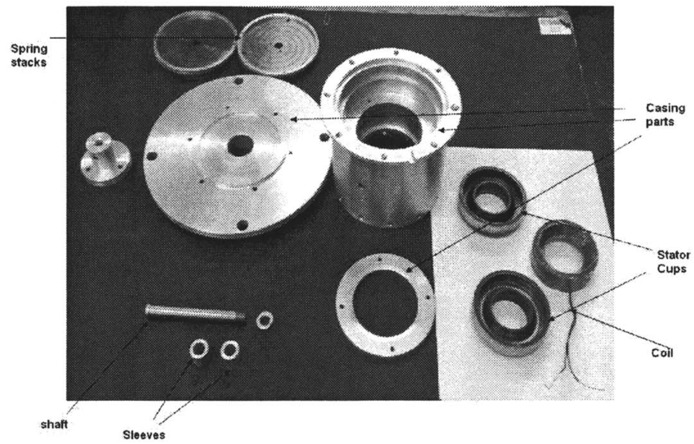

Figure 4: Motor casing components

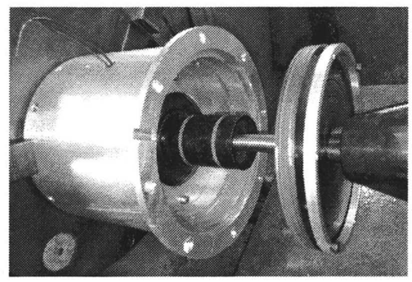

Figure 5: Accommodating mover and stack into the case

4 Test Results

4.1 Thermal results

To measure the temperature rise in the winding due to ohmic loss the average winding temperature has been deduced from rate of resistance change with temperature monitored every 5 seconds for 2 hours. The curve of the temperature variation in the coil is shown in Fig. 6 when excited with 1A. This reveals a steady state temperature rise of 13 deg C which indicates a current rating for 100degC rise of 2.8A. The intended rated current is 2A which will probably be within thermal limits when running fully loaded and incurring iron loss (these tests have yet to be done).

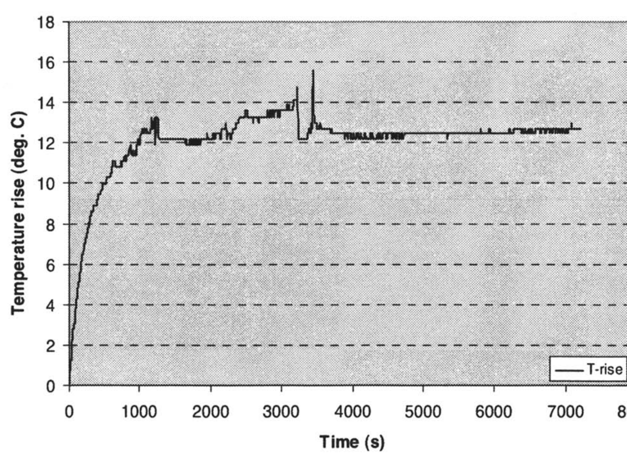

Figure 6: Temperature variation in the windings (measured)

4.2 Resonance frequency and damping tests

The mechanical equation governing the motion at free oscillation can be expressed as

$$M \frac{d^2 x}{dt^2} + D \frac{dx}{dt} + Kx = 0 \qquad (1)$$

From the equation the mechanical resonance frequency and the damping factor can be defined as

$$\omega_n = \sqrt{\frac{K}{M}} \qquad (2)$$

$$\xi = \frac{D}{2\sqrt{KM}} \qquad (3)$$

The mechanical resonance frequency is an essential parameter for oscillating linear motors as their efficiency is optimum when its mechanical system resonates at the electrical supply frequency. From the design parameters shown in table 1, the mechanical resonance frequency can be determined and it is 47.1 Hz without including the mass of the force sensor as the free damped oscillation was done without it. Including the force and the displacement sensors in the whole system back to back motors gives a theoretical value of 46.5 Hz for the mechanical resonant frequency of the system.

Mass of the mover	0.385 kg
Mass of the force sensor	0.045 kg
Mass of the position sensor	0.002 kg
Effective mass of the springs	0.317 kg
Spring stiffness, K at x=2mm	70000 N/m

Table 1: Mechanical parameters of the motor

Another important parameter for this type of system is the damping factor which is used in equation (3) to calculate the "friction" coefficient that is used in equation (1) to analyse the mechanical behaviour of the motor. In this case the "friction" is made up from mechanical losses in the springs, windage and iron loss in the SMC. A test was done in which the mover/spring system was mechanically displaced and then suddenly released. The output form the linear variable transformer position sensor (LVDT) is shown in Fig.7. In these systems a high frequency signal (5kHz) is induced into a secondary such that the magnitude of the signal in the secondary is proportional to position. In Fig 7 the initial displacement is shown from the large signal size at the left of the figure and the vibration is evident in the modulation (at the resonant frequency) of the 5kHz signal. The sensor is traversing close to its zero position so the smaller peaks are actually the deflection to the opposite side from the initial deflection. From these results the resonant frequency and the damping factor ξ can be calculated and hence the friction coefficient D. It is found from the envelope of the signal that the resonant frequency is about 49 Hz which is in acceptable range as compared to the calculated frequency, 47.1 Hz. Moreover, it is found from the decay of signal magnitude that the damping factor ξ is 0.007 as explained in Fig. 8 and hence the "friction" coefficient can be calculated and it is 3.3 Ns/m. As may be evident from Fig. 7 the damping is small (implying low losses when running)

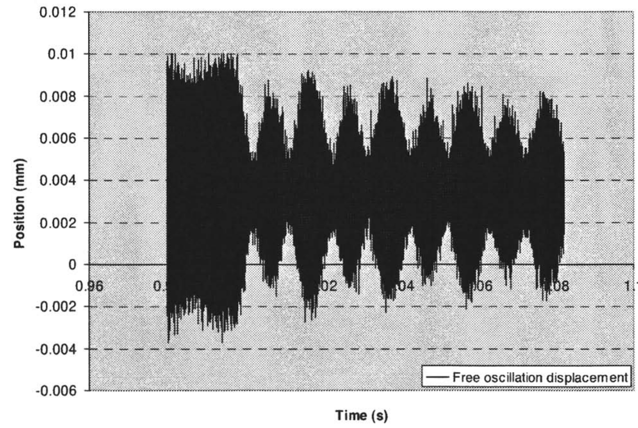

Figure 7: Free damped oscillation of the motor

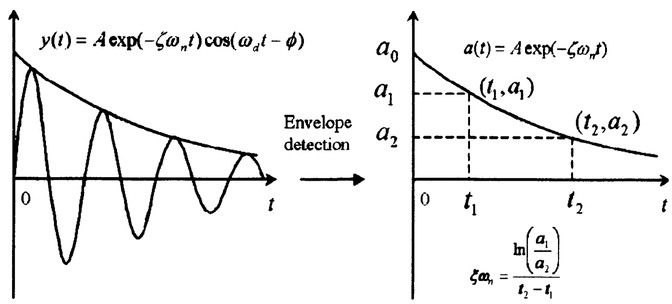

Figure 8: Damping factor ξ determination [9]

4.3 Static test results

In order to validate the method that has been used to design the motor, FE, some static tests have been done. The test rig is shown in fig. 8. Firstly, resistance and inductance were measured by exciting the machine with 50Hz ac with the mover clamped. In such a test losses will be caused in the SMC (iron loss) and magnets (eddy currents) and hence a higher resistance and (slightly) lower inductance are to be expected. As shown in table2.

	Measured	Calculated
Resistance, R (ohm)	13.2	10.4
Inductance, L (H)	0.38	0.41

Table 2: Electrical parameters of the motor

Static force against position is found by displacing the mover and applying a range of currents. At zero position (mover at the centre), the motor provides the only force while the spring force and the magnetic centring force caused by the magnets acting alone are also involved when the shaft moves from the centre. Fig. 9 shows a good agreement between the FE and the experimental static forces at the centre when varying DC currents from -2A to 2A by a step of 0.5A.

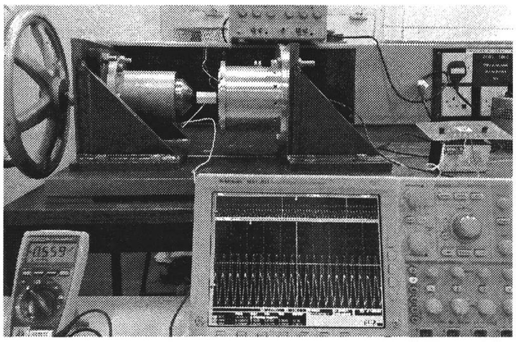

Figure 9: Static force against dc current test rig

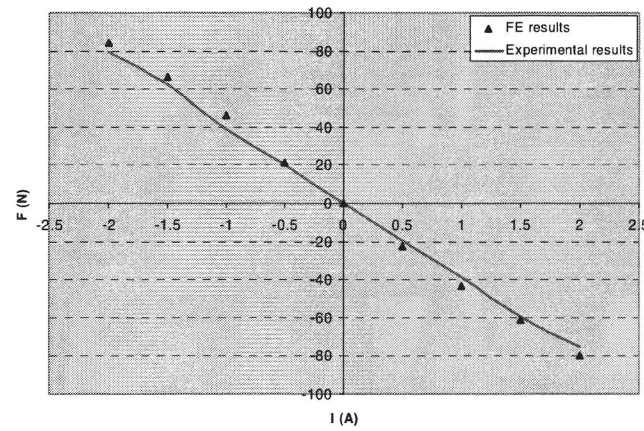

Figure 10: FE and Experimental F-I curve

The forces from the springs are far larger than the force generated by the motor (in the region of 10 times). This causes a force sensor range problem as it is chosen to measure only the resultant force and hence displacement is limited to +/- 6mm. The results show good agreement with the calculated results (which are themselves the sum of two FE calculations for the mechanical and the magnetic systems respectively) when 2A, 0A and -2A currents were applied as can be seen from Fig. 11. One detail to note in Fig. 11 is that the springs are not quite linear – the spring rate increases slightly with deflection. This is a natural property of the flexure springs used and it results in a slightly different resonant frequency (i.e. rising) as the deflection increases. This property is clearly important when designing for a compressor application. Getting the total system as near resonant as possible is of key importance to efficiency and it may be that the spiral springs as they are currently designed are not sufficiently linear with the key question being the range of stroke necessary.

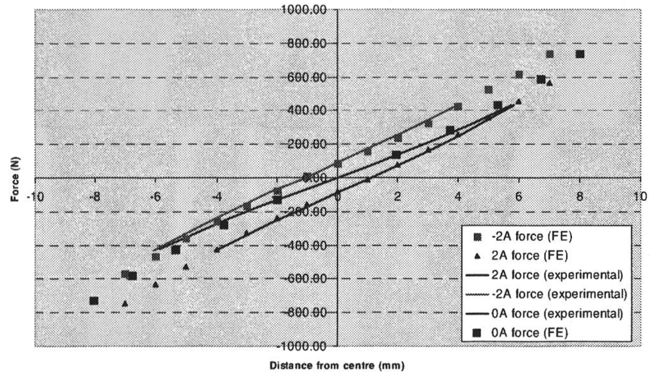

Figure 11: Static forces including springs force

The comparison between the experimental and calculated results in both figures 10 and 11 is good lending confidence to the design methods used.

4.4 Dynamic test results

A single motor has been supplied with 50Hz ac over a range of voltages (and hence deflections) with the mover running free. The tests to date have been problem free lending confidence to the mechanical arrangement. Current, power and displacement were then measured. Fig.12 shows that the measured current and displacement agree reasonably with the calculated results.

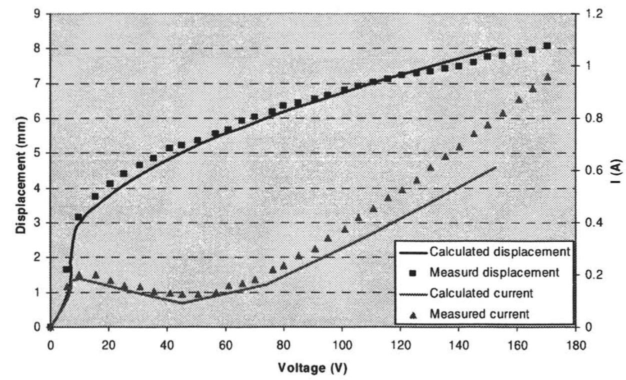

Figure 12: Calculated and measured current and displacement against driving voltage

The equations for this system are

$$v = iR + L\frac{di}{dt} + \frac{d\varphi}{dx}\frac{dx}{dt} \tag{4}$$

$$M\frac{d^2x}{dt^2} + D\frac{dx}{dt} + Kx = \frac{d\varphi}{dx}i \tag{5}$$

Given a fixed mechanical (M, D, K) and electrical (dφ/dx, R and L) constants a given magnitude of vibration (with frequency fixed at 50Hz) will require a corresponding and proportional current. The voltage is proportional to current and movement hence the required voltage is also proportional to movement. The results shown in Fig 12 are clearly far from that and the reason is the increase in stiffness with the size of the deflection. The calculated results in Fig. 12 were done using the calculated parameters and hence the stiffness increases with deflection as predicted by the mechanical FE results. This makes resonance occur at 50Hz at around a movement of 5mm peak/peak and is the reason for the current minimum at that deflection. This is further reinforcement of the need for accurate setting of the resonant frequency and highlights the difficulty if the spring stiffness changes significantly.

Total power loss P_{total} has measured via a power analyser and hence its different parts i.e. copper, friction and iron losses can be calculated from the following equations:

$$P_{copper} = i^2 R \tag{6}$$

$$P_{friction} = \frac{1}{2} D \cdot x^2 \cdot \omega^2 \tag{7}$$

$$P_{iron} = P_{total} - P_{copper} - P_{friction} \tag{8}$$

Fig.13 shows the curves of the different power losses against the driving voltage.

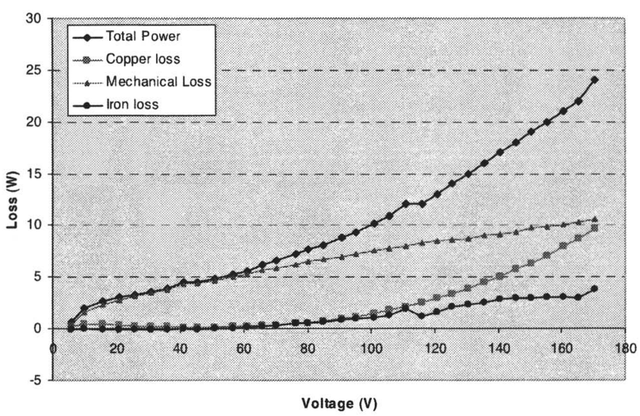

Figure 13: Different power losses against voltage

The two back to back motors (motor-generator) arrangement is, shown in Fig.14 just before their coupling both sensors are clear in the figure, the force sensor will be hidden after the coupling.

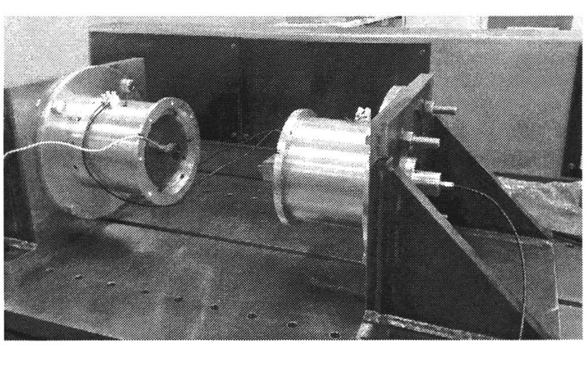

Figure 14: Motor- generator arrangement just before coupling

5 Conclusions

A single phase permanent magnet linear motors with a flux concentrating buried magnet arrangement has been designed and two identical motors have been constructed utilising Somaloy® 700 +0.4% Kenolube SMC. One motor has been tested statically and then dynamically. From static tests, force measurements against position and current, which describe the thrust capability of the machine, have been shown. The mechanical resonant frequency and the damping factor have been estimated from the free damped oscillation. Finally, current, power and displacement were shown from running tests showing good agreement with predicted results.

References

[1]P. Bucherot, "Appareils et machines a courant et mouvememt alternatifs" *Bulletin de la Societe Internationale des Electriciens*, Paris, pp 731-755 (1908).

[2] R. E. Clark, D. S. Smith, P. H. Mellor and D Howe, "Design optimisation of moving-magnet actuators for reciprocating electro-mechanical systems" *IEEE transaction of Magnetics*, **vol. 31**,No. 6, pp. 3746-3748 (1995).

[3]K. Kim, D. Kim, Y. Song and J Kim, "Linear compressor" *US Patent* no. 20040247457A1, 2004.

[4]J. Wang, W. Wang, G. Jewell and D. Howe, "Design and experimental characterisation of a linear reciprocating generator" *IEE Proceedings of Electrical Power Application*, **vol. 145**, No. 6, pp. 509-518 (1998).

[5] J. Wang and D. Howe, "Influence of soft magnetic material on the design and performance of tubular permanent magnet machines" *Proc. INTERMAG Conference*, Nagoya, Japan, , pp.813-814 (2005).

[6] A. G. Jack, Z. S. Al-Otaibi and M. Persson, " Alternative designs for oscillating linear single phase permanent magnet motors using soft magnetic composites", *Proceedings of International Conference on Electrical Machines and Systems,(ICEMS2006)*, Nagasaki, Japan, (2006).

[7] Z. Al-Otaibi and A. G. Jack, "Spiral flexure springs in single phase linear-resonant motors" *Proceedings of UPEC2007*, Brighton, UK, pp 184-187 (2007)

[8]Somaloy™ 700, *Hogana AB(publ)*, S-263 83 Hoganas, Sweden.

[9]K. Zeng and C. A. Grimes, "Threshold-crossing counting technique for damping factor determination of resonator sensors", *Review of Scientific Instruments*, **vol. 75**, No12, pp. 5257-5261(2004).